J. Aerosol Sci., Vol. 22, No. 7, pp. 843–867, 1991.
Printed in Great Britain.

0021-8502/91 $3.00+0.00

CORRECTION FOR SAMPLING ERRORS DUE TO COAGULATION AND WALL LOSS IN LAMINAR AND TURBULENT TUBE FLOW: DIRECT SOLUTION OF CANONICAL 'INVERSE' PROBLEM FOR LOG-NORMAL SIZE DISTRIBUTIONS*

DANIEL E. ROSNER† and MENELAOS TASSOPOULOS

Yale University, Department of Chemical Engineering, High Temperature Chemical Reaction Engineering Laboratory, New Haven, CT 06520-2159, U.S.A.

(*Received* 22 *February* 1991; *and in final form* 24 *June* 1991)

Abstract—Aerosol sampling from industrial environments (e.g. combustion engines) or natural environments (e.g. the troposphere) frequently involves conveying the sample to a downstream ('sheltered') instrument via an upstream tube or duct. While the instrument may be capable of characterizing, say, the particle size distribution (PSD) of the aerosol actually presented to it, the investigator is, of course, usually more interested in the PSD of the aerosol entering the upstream sampling tube. Invariably, this differs from that measured because of several systematic phenomena—perhaps the two most obvious of which are particle size-dependent losses to the tube walls (i.e. incomplete 'penetration') and PSD distortion due to suspended particle–particle coagulation when the particle concentrations are sufficiently high. We show here how recent research on the use of 'moment methods' to predict the effects of size-dependent walls loss and/or Brownian coagulation in flow systems can now be brought to bear to conveniently solve this 'inverse' problem by numerically integrating the quasi-one-dimensional coupled moment equations in the upstream direction, using downstream (measured) aerosol properties in the definitions of all dimensionless dependent variables and parameters. Illustrative 'universal' graphs are presented here for the sampling of log-normally distributed 'inertialess' (Brownian) aerosols in long straight adiabatic ducts for both commonly encountered extremes of particle Knudsen number $\mathrm{Kn}_p \gg 1$(free molecule) or $\mathrm{Kn}_p \ll 1$ (continuum), as well as convenient rational approximations derived from the leading terms of a Taylor series expansion of the above-mentioned dimensionless moment equations.

NOMENCLATURE

A	cross-sectional area of duct
b	exponent describing dependence of St_m on particle volume v
C	dimensionless coagulation rate parameter (fm or c)
C_f	friction factor (dimensionless wall shear stress)
$C_1^{(k)}$	first order coefficient in Taylor series expansion of $M_k(\xi)$
d_g	particle diameter corresponding to v_g
D	Brownian diffusion coefficient for particle of volume v
d_w	duct diameter
$f_k(u, v)$	function of particle volumes appropriate to moment k
F_k	dimensionless moment shift function (equation (12))
$\bar{F}_e$	entrance effect correction for streamwise averaged mass transfer coefficient
k	moment index (e.g. $k = 0, 1, 2$ are of particular physical interest)
k_B	Boltzmann constant; Table 2
K	environment/mechanism-dependent part of the coagulation rate constant β
Kn_p	Knudsen number based on prevailing gas mean-free path and particle diameter
L	total length of sampling duct (upstream of detector)
m_p	mass of particle of volume v
M_k	k^{th} moment of $n(v, \ldots) \equiv \mathrm{d}N_p/\mathrm{d}v$
n	size distribution function $\mathrm{d}N_p/\mathrm{d}v$
N_p	total particle number density ($\equiv M_0$)
Nu_m	mass transfer Nusselt (Sherwood) number (Rosner, 1986)
P	'wetted' perimeter of the duct of cross-sectional area $A(z)$

* Supported, in part, by AFOSR (Grand 89-0223), DOE-PETC (Grant DE-FG-22-9 0PC90099) and the 1991 Yale HTCRE Lab Industrial Affiliates (Union Carbide, Shell, SCM Chemicals, DuPont, General Electric).
† Professor of Chemical Engineering, Yale Univ.; Director HTCRE Lab.

Re Reynolds number based on $4A/P$ and mean velocity U
R radius (of curvature) of centerline of a bend (e.g. elbow) in duct
Sc particle Schmidt number $(\mu/\rho)_{gas}/D$
St_m mass transfer Stanton number, $Nu_m/(ReSc)$ (Rosner, 1986)
t time
t_p particle stopping time in the prevailing carrier gas
t_p^+ $u_*^2/t_p/\nu$; dimensionless particle stopping time
T absolute temperature (K)
U mean velocity of carrier gas in sampling duct
u particle volume (dummy variable)
u^* friction velocity $(C_f/2)^{1/2}U$
v volume of spherical particle
v_g geometric-mean particle volume in log-normal PSD $n(v, \ldots)$
$\bar{v}$ mean particle volume, ϕ_p/N_p, of local aerosol
x $L - z$; distance measured upstream from the detector
$\mathbf{x}$ position vector
z distance measured downstream from the sampling tube inlet
$Z^{(k)}$ collision integral functions defined by coagulation rate law (equation (15))

Greek letters

β coagulation rate constant in "mass-action" law (equation (14))
ξ scaled dimensionless distance upstream of the aerosol detector
ϕ_p particle volume function ($\equiv M_1$)
ρ_p intrinsic density of a particle (m_p/v_p)
μ_k dimensionless k^{th} moment of PSD ($\mu_0 = 1$, $\mu_1 = 1$)
μ_{gas} dynamic Newtonian viscosity of the carrier gas
ν momentum diffusivity of the carrier gas, μ_{gas}/ρ_{gas}
ζ_m $(ReSc)^{-1}(L/d_w)$ (in equation (40))
σ_g geometric standard deviation of the log-normal PSD $n(v, \ldots)$ (see, e.g. Rosner and Tassopoulos, 1989)

Subscripts and superscripts

C pertaining to interparticle coagulation
c coagulation
eff effective
k pertaining to moment k where k need *not* be an integer nor positive
(k) pertaining to moment k
g pertaining to log-normal PSD (geometric)
gas pertaining to the carrier gas
L evaluated at $z = L$ (downstream location of aerosol detector)
max maximum value
meas measured
p particle(s)
o evaluated at the sampling system inlet station ($z = 0$)
WL pertaining to wall loss
$'$ first derivative with respect to ξ
$''$ second derivative with respect to ξ

Others

$\tilde{(\ )}$ normalized by the value $(\ )$ at the aerosol detector (at $z = L$)
$\bar{(\ )}$ mean value (e.g. $\bar{v} \equiv \phi_p/N_p$, $\bar{d} = (6\bar{v}/\pi)^{1/3}$; $\overline{St}_m$ (streamwise mean))

Abbreviations

c continuum ($Kn_p \ll 1$)
coag pertaining to (caused by) coagulation
fm free molecule ($Kn_p \gg 1$)
GDE general dynamic equation (population balance)
h.o.t. higher order terms
ODE ordinary differential equation
PSD particle size (volume) distribution
RHS right hand side (of equation)
WL pertaining to (caused by) particle loss to walls

1. INTRODUCTION, BACKGROUND AND MOTIVATION

Historically, the need to accurately sample industrial and natural aerosols has led to many advances in the science and technology of fine particulate matter suspended in gases, including the invention and development of a wide variety of clever instruments as well as

ancillary theoretical developments concerning techniques for avoiding or minimizing 'bias' when extracting the sample and delivering it to the instrument (see, e.g. Fuchs, 1964; Davies, 1966; Mercer, 1973; Friedlander, 1977; Hinds, 1982; Hidy, 1984; Vincent, 1989). Some phenomena will cause an unavoidable systematic 'distortion' in the recorded particle size distribution (PSD) which must be corrected for—in particular—the size-dependent loss of particles to the walls of an upstream sampling tube, and any suspended particle–particle coagulation that occurs between the inlet of the sampling tube and the (downstream) monitoring instrument. The present contribution provides rational, yet simple, methods to make such corrections, under conditions that, while deliberately idealized, are frequently encountered. Indeed, one of our goals is to produce a set of generalized graphs which can facilitate making such corrections for Brownian aerosols (in the absence of appreciable inertial- and sedimentation-phenomena), as well as guide the design/selection of sampling systems which will keep future corrections acceptably small.

Wall deposition losses in the absence of interparticle coagulation have been the subject of many early investigations, especially for the case of dilute, steady, fully-developed laminar gas flow in straight, constant-area ducts (see, e.g. Fuchs and Sutugin, 1971). This understanding, in fact, led to the development of the so-called 'diffusion battery' (see, e.g. Mercer and Green, 1974) for estimating PSDs based on the observed penetration characteristics of the aerosol as a function of particle size, duct diameter, length, and gas flow rate. At suspended particle concentrations high enough for non-negligible coagulation (Brownian, shear, . . .) the situation becomes rather more complicated and the computational methods used by earlier investigators to predict PSD distortion effects fail (i.e. assuming that the penetration of one particle size class is not influenced by the simultaneous presence of the others). Indeed, the interesting interactions between coagulation and convective-diffusion deposition rates now comprise an active field of research (see, e.g. Park and Rosner, 1989; Pratsinis and Kim, 1989; Bai and Biswas, 1990; Rosner and Tassopoulos, 1990), to which the present paper contributes. The present work is also an extension and application of techniques we have recently developed for predicting total mass deposition rates from polydispersed aerosol populations formed by coagulation (Rosner, 1989; Rosner and Tassopoulos, 1989), but without the complication of appreciable coagulation within diffusion boundary layers (see, e.g. Park and Rosner, 1989; Bai and Biswas, 1990).

Finally, mention should be made of relevant theoretical studies whose primary purpose was to support/interpret fundamentally-oriented experiments on the mechanisms of organic- and inorganic-soot production in laminar flames (see, e.g. Ulrich and Subramanian, 1977; Ulrich and Riehl, 1982; Dobbins and Mulholland, 1984; Dobbins and Megaridis, 1987; Frenklach and Harris, 1987; Megaridis and Dobbins, 1990; Megaridis, 1987; Zachariah and Semerjian, 1989). Indeed, our treatment below of free-molecule regime coagulation in aerosol sampling system *is* equivalent to that of Dobbins and Mulholland (1984) (rather than that of Lee *et al.*, 1984), suitably augmented to include the simultaneous occurrence of particle size-specific convective-diffusion to the walls of the sampling tube.

Rather than explicitly dealing with the 'direct' problem of predicting the 'evolution' of the penetrating (and depositing) aerosol as a function of dimensionless downstream distance and coagulation parameters (see, e.g. Rosner and Tassopoulos, 1990, 1991b) we show here (section 3.6) that by 'backwards' (upstream-) integration of the governing moment equations and the use of dimensionless dependent variables and parameters based on downstream reference quantities, we, in effect, can provide direct solutions to the canonical 'inverse' problem of aerosol sampling theory—i.e. correction factors which allow the investigator to go immediately from PSD-parameters recorded at the downstream instrument to the PSD-parameters that must have characterized the aerosol entering the inlet* of the sampling

* Additional correction factors may be necessary due to peculiarities of the inlet orifice itself, and its geometric surroundings (see, e.g. Vincent, 1989; Mercer, 1973; Hungal and Willeke, 1990 ; Belyaeu and Levin, 1974; Zabel, 1978; Ivie *et al.*, 1990; Huebert *et al.*, 1990). In considering the need for such additional factors, however, the reader should bear in mind that we emphasize here Brownian particles well below the 'inertial' range. In any case, if necessary, additional 'inlet' correction factors can be superimposed on the present predictions.

tube. Toward this end, in section 2 we spell out our underlying assumptions/idealizations, and in section 3 we state the laws used here to predict the evolution of the three lowest integral moments of the log-normal shape aerosol PSD for (quasi-) steady, (quasi-) one-dimensional gas flow in a straight adiabatic aerosol sampling duct. General results ('universal' graphs and formulae) are presented in section 4, together with a simple numerical ('backward-marching') procedure for dealing with much more complex cases. Some implications and applications of the results of section 4 are provided and briefly discussed in section 5 with the help of two specific numerical air-monitoring examples (nearly isothermal)—one ground-based and one airborne. Section 6 offers a concise defense of many useful idealizing assumptions, as well as an indication of how to relax many of the assumptions exploited here for particular sampling applications which are more complex, such as extractive sampling from high temperature combustors (for further details the reader is referred to the references cited in section 6 and Rosner and Tassopoulos (1990, 1991b)). Our summary recommendations, and an indication of future relevant work are contained in section 7, which concludes the present paper. Extensions based, in part, on section 6 will be the subject of future communications from this laboratory.

2. BASIC ASSUMPTIONS

In keeping with our goal of deriving reasonably general results applicable to a wide variety of intrinsically similar, commonly encountered sampling situations we introduce the following explicit simplifying assumptions and idealizations. These are defended or shown to be relaxable in section 6.

A1: Quasi-one dimensional steady gas flow in a straight adiabatic sampling duct with constant effective diameter $d_{\text{eff}} = 4A/P$.

A2: Aerosol PSD well-represented by a single mode continuous log-normal function of the dense spherical particle volume v.

A3: Axial *diffusion* of particles negligible compared to axial *convection*.

A4: Previously calculated (or measured) fully-developed perimeter-averaged mass transfer coefficients adequately describe local convective-diffusion particle mass transport to the wall, and depend on a single power, b, of the particle volume valid in the high Schmidt number ($\text{Sc} = \nu/D_p \gg 1$) limit.

A5: Negligible interfacial 'barrier' to incident particle capture by the wall, and negligible reentrainment of already deposited particles.

A6: Brownian coagulation occurs primarily in the core of the sampling duct flow according to the mass-action laws of free-molecule transport ($\text{Kn}_p \gg 1$) or continuum transport ($\text{Kn}_p \ll 1$).

As discussed in section 6, Assumptions A3, A4, and A6 can apply to either laminar or turbulent duct flow (perhaps more accurately to the latter than the former (because of A4, see sections 5.2 and 6)). Methods to include the systematic consequences of 'entry' effects, non-power-law deposition, transition regime particle transport and coagulation, diabatic walls, bends (in a 'piecewise-straight' sampling system) and non-spherical 'aggregated' solid particles are taken up briefly in section 6, and in greater detail in Rosner and Tassopoulos (1990, 1991). It should also be remarked that in the continuum limit ($\text{Kn}_p \ll 1$) many of our methods/results will apply to particle suspensions in flowing *liquid* (hydrosals).

3. MOMENT METHODS AND LOG-NORMAL PSDs

Rather than dealing directly with the complete suspended particle population balance or 'general dynamic equation' (GDE) governing the continuous size distribution function $n(v, \mathbf{x}, t) = \mathrm{d}N_p/\mathrm{d}v$ (presumed to be measurable at the location of the downstream aerosol instrument) the predictions made below are based on solving a closed set of coupled

differential equations for the three lowest integral 'moments' of $n(v, \ldots)$, defined by:

$$M_k \equiv \int_0^\infty v^k n(v, \ldots) \mathrm{d}v \qquad (k = 0, 1, 2). \tag{1}$$

This strategy, and its implementation for the case of steady quasi-one dimensional duct flow, are the subjects of sections 3.1–3.6 below. Owing to more extensive discussions elsewhere (see, e.g. the mass deposition-oriented work of Rosner, 1989; Rosner and Tassopoulos, 1989, 1990, 1991) only the most important conclusions/results are stated below for completeness.

3.1. *Method of moments*

The use of differential equations for the moments of $n(v, \ldots)$ to construct rational approximate solutions to the GDE (an integro–differential equation) is a subject that has been under intense development in the past two decades, and progress continues unabated. Moment methods have been especially successful in elucidating many aerosol situations involving coagulation (see, e.g. Cohen and Vaughn, 1971; Lee *et al.*, 1984; Dobbins and Mulholland, 1984; Megaridis and Dobbins, 1989, 1990; Pratsinis and Kim, 1989; Frenklach and Harris, 1987, . . .). Although different authors use somewhat different methods to achieve closure, especially when coagulation occurs near or in the 'free-molecule' regime, almost all authors derive/use equations for M_0, M_1, and M_2, which are, indeed, particularly simple (see sections 3.4 and 3.5). The first two moments also have the merit of being of direct physical significance, with $M_0 = N_\mathrm{p}$ (the total particle number density) and $M_1 = \phi_\mathrm{p}$ (the total particle volume fraction). In the present case of steady quasi-one-dimensional flow in a sampling duct we therefore focus our attention on the coupled ordinary differential equations governing the $M_k(z)$, where $k = 0, 1, 2$, and z is the axial coordinate down the sampling tube (measured from the inlet). When use is made of the known laws of particle deposition (section 3.4) we encounter terms involving additional moments M_k, where $k \neq 0, 1, 2$ so that it becomes necessary to interrelate moments to obtain a closed set of integrable equations. In the present case this is accomplished using the log-normal PSD shape approximation, as discussed in section 3.2, and defended in section 6 for this class of problems.

3.2. *Implications of log-normality*

It is now well known that 'coagulation-aged' populations of aerosol particles closely approach single-mode log-normal size distributions (i.e. Gaussian in $\ln(v)$). Moreover, it is easy to demonstrate that power-law wall removal processes (see A4 and section 3.3) will not alter this situation. Hence, for our present purposes the single-mode log-normal approximation is a particularly appropriate and convenient starting point. For such single-mode log-normal PSDs it can also be shown that all moments are necessarily interrelated as follows:

$$M_k = v_\mathrm{g}^k \cdot N_\mathrm{p} \cdot \exp\left(\left(\frac{k^2}{2}\right) \ln^2 \sigma_\mathrm{g}\right), \tag{2}$$

where v_g is the median (geometric mean) particle volume and σ_g is the corresponding geometric standard deviation of the PSD. These PSD parameters can be related to N_p, ϕ_p, and M_2 *via*:

$$\ln^2 \sigma_\mathrm{g} = \ln\left(\frac{M_2 \cdot N_\mathrm{p}}{\phi_\mathrm{p}^2}\right) \tag{3}$$

and

$$v_\mathrm{g} = \left(\frac{\phi_\mathrm{p}}{N_\mathrm{p}}\right)^{3/2} \cdot (M_2)^{-1/2} \tag{4}$$

but any other desired moment $M_k (k \neq 0, 1, 2)$ can now be obtained in terms of either N_p, ϕ_p, and M_2, or N_p, v_g and σ_g. We will also have frequent need for the relation:

$$v_g = \bar{v} \cdot \exp\left(-\left(\frac{1}{2}\right)\ln^2 \sigma_g\right), \tag{5}$$

where $\bar{v} \equiv \phi_p / N_p$ is the mean particle volume.

While not discussed further here, the assumption of log-normality in effect also allows us to escape the numerical problems often encountered in 'inverting' aerosol population measurements (see, e.g. Cooper and Wu, 1990). Thus, our "upstream" integrations (section 3.6) are perfectly straightforward, but deliberately limited to cases where the required PSD-parameter 'correction' factors are well within one decade of unity.

3.3. *Modeling particle size-dependent particle wall losses*

For steady quasi-one-dimensional (z-direction) flow in a duct of area $A(z)$ and wetted perimeter $P(z)$ the wall loss contribution can be written (see, e.g. Rosner and Tassopoulos, 1990)

$$\left\{\frac{1}{A}\frac{d}{dz}(AUM_k)\right\}_{\text{wall loss}} = -\frac{P}{A}U \cdot \int_0^\infty \text{St}_m(v) \cdot v^k n(v)\, dv, \tag{6}$$

where $\text{St}_m(v)$ is the appropriate perimeter-mean particle volume-dependent dimensionless mass transfer coefficient (Stanton number = $\text{Nu}_m/(\text{ReSc})$), Rosner (1986) at station z, and $n(v, z)$ is the PSD describing the bulk (mixing-cup averaged) suspended particle–gas mixture at this same streamwise station. As shown and exploited in our recent work (see, e.g. Rosner, 1989; Rosner and Tassopoulos, 1989) in the submicron particle size range of primary interest here it is often possible to accurately represent the v-dependence of $\text{St}_m(v, \ldots)$ by simple power-law:

$$\text{St}_m \cong \text{St}_m(\bar{v}) \cdot \left(\frac{v}{\bar{v}}\right)^b \tag{7}$$

where, e.g. for $\text{Sc} \gg 1$ turbulent convective-diffusion (see, e.g. Rosner (1986, 1990) equation (6.5–11b)) $\text{Nu}_m \sim \text{Sc}^{0.296}$, $\text{St}_m \sim \text{Sc}^{-0.704}$ and therefore:

$$b = 0.704\left(\frac{\partial \ln D}{\partial \ln v}\right) \tag{8}$$

and, for fully-developed laminar flow $\text{Nu}_m = \text{const}$, $\text{St}_m \sim \text{Sc}^{-1}$, so that:

$$b = \left(\frac{\partial \ln D}{\partial \ln v}\right). \tag{9}$$

Since $D \sim v^{-2/3}$ for dense spherical particles in the free-molecule regime ($\text{Kn}_p \gg 1$), and $D \sim v^{-1/3}$ for dense spherical particles in the continuum limit, the exponents b used in our calculations below are readily obtained and summarized in Table 1. For isothermal convective-diffusion they are seen to fall between the extremes of -0.235 and -0.667. Other mechanisms of particle transport to the sampling tube wall (e.g. eddy impaction, or particle thermophoresis) and other types of particles (e.g. aggregates comprised of smaller diameter 'primary' particles) will, of course, be characterized by rather different b-values, as discussed elsewhere (Rosner, 1989; Rosner and Tassopoulos, 1989; Rosner, 1991).

Taking into account this power-law behavior, and considering the particular case of constant area adiabatic duct flow, we find that equation (6) can be simplified to:

$$\left\{U\frac{dM_k}{dz}\right\}_{\text{wall loss}} = -\frac{P}{A}U \cdot \text{St}_m(\bar{v}) \cdot \bar{v}^{-b} \cdot M_{k+b}, \tag{10}$$

where, in the equations below $k = 0, 1, 2$. In practice (see, e.g. section 3.5) we rewrite

Table 1. Values of the exponent b for fully-developed convective diffusion in straight ducts

	Flow regime	
Particle Knudsen number	Laminar*	Turbulent†-smooth wall
Free-molecule (fm)	−2/3	−0.469
Continuum (c)	−1/3	−0.235

* In this case $Nu_m \sim$ constant so that $St_m \sim Sc^{-1}$.
† Based on $Sc \gg 1$ transport by Brownian motion within the viscous sublayer.

equation (10) in the formally simple way:

$$\left\{U\frac{dM_k}{dz}\right\}_{\text{wall loss}} = -\frac{P}{A}U \cdot St_m(\bar{v}) \cdot F_k \cdot M_k, \tag{11}$$

where F_k is the dimensionless 'moment-shift' function* defined by:

$$F_k \equiv \frac{\bar{v}^{-b}M_{k+b}}{M_k} = \frac{\mu_{k+b}}{\mu_k} \tag{12}$$

where we have introduced the dimensionless moments:

$$\mu_k \equiv \exp\left\{\frac{k(k-1)}{2} \cdot \ln^2 \sigma_g\right\}. \tag{13}$$

Equations (12) and (13) follow from the PSD-condition of log-normality.

3.4. *Inclusion of coagulation processes at high particle number densities*

If the coagulation rate between $n(v)dv$ particles/volume of volume $v \pm dv/2$ and $n(u)du$ suspended particles/volume of volume $u \pm du/2$ is taken to be of the 'mass-action' form $\beta(u, v)n(u)n(v)du\,dv$ then it is known that (in a well-mixed, transient situation):

$$\left(\frac{dM_k}{dt}\right)_{\text{coag.}} = \frac{1}{2}\int_0^\infty \int_0^\infty f_k(u, v) \cdot \beta(u, v)n(v) \cdot n(u)\,dv\,du. \tag{14}$$

Clearly $f_0 = -1$ and $f_1 = 0$, and it can be shown that $f_2 = 2uv$ (see, e.g. Cohen and Vaughn (1971)). Following Dobbins and Mulholland (1984), for log-normal distributions, once the rate constant $\beta(u, v)$ is specified the right-hand side of equation (14) can always be calculated numerically and the results expressed in the form:

$$\left(\frac{dM_k}{dt}\right)_{\text{coag.}} = \frac{1}{2}K \cdot N_p^2 \cdot Z^{(k)}(v_g, \sigma_g), \tag{15}$$

where the coefficient K is independent of particle size and number density but dependent on environmental conditions and perhaps particle material properties. Values of K and the so-called collision integrals $Z^{(k)}$ for the free-molecule (fm) coagulation of hard spheres (Dobbins and Mulholland, 1984) are reproduced (in our notation) in the top rows of Table 2. In the continuum (c) limit it is well known that $(dM_0/dt)_{\text{coag}}$ is proportional to $-(M_0^2 + M_{1/3}M_{-1/3})$ and $(dM_2/dt)_{\text{coag}}$ is proportional to $(M_1^2 + M_{4/3}M_{2/3})$ (see, e.g. Cohen and Vaughn (1971) or Flagan and Seinfeld (1988)) with the proportionality constant (hence K-value) depending on the combination $k_B T/\mu_{\text{gas}}$. When these results are recast in terms of equation (15) using equation (5) we obtain/use the values of K_c and $Z_c^{(k)}$ shown in the bottom row of Table 2. Thus, in the equations below we set the Brownian coagulation contribution to $U dM_k/dz$ equal to the RHS of equation (15), and, for $\sigma_g < 3.32$, used the

* In our previous papers (Rosner, 1989; Rosner and Tassopoulos, 1989) particular attention was focused on F_1 $(= \mu_{1+b})$, which was shown to be equal to the physically interesting ratio of the actual total mass deposition rate to the total mass deposition rate if all particles in the population had the mean volume $\bar{v}$.

Table 2. Summary of factors*†‡ appearing in the coagulation rate term [equation (15)]

Coagulation regime§	$K(T, \ldots)$	$Z^{(0)}$	$Z^{(1)}$	$Z^{(2)}$
Free-molecule*($\mathrm{Kn_p} \gg 1$)	$\left(\frac{3}{4\pi}\right)^{1/6} \cdot \left(\frac{6k_B T}{\bar{\rho}_p}\right)^{1/2}$	$-4\sqrt{2}v_g^{1/6} \cdot \exp\left[\frac{3}{16}\ln^2\sigma_g\right]$	0	$8\sqrt{2}v_g^{13/6} \cdot \exp\left[\frac{65}{48}\ln^2\sigma_g\right]$
Continuum ($\mathrm{Kn_p} \ll 1$)	$\frac{4k_B T}{3\mu_{gas}}$	$-2\left\{1+\exp\left(\frac{1}{9}\ln^2\sigma_g\right)\right\}$	0	$4v^2 \cdot \left[1+\exp\left(\frac{1}{9}\ln^2\sigma_g\right)\right]$

* Values taken from Dobbins and Mulholland (1984); see, also, Megaridis and Dobbins (1990a) for $\sigma_g > 3.32$.

† As a consequence of the assumed conservation of volume when two particles collide and coalesce $Z^{(1)}$ vanishes for all cases. (Recall that $M_1 = \phi_p$ = particle volume fraction.)

‡ Note that, according to equation (15) only the products $KZ^{(k)}$ necessarily have the same dimensions (in the fm and c cases). However, as is clear from the entries above, the K-factors (and the corresponding $Z^{(k)}$ factors) themselves do not have the same dimensions in the free-molecule and continuum cases.

§ For intermediate $\mathrm{Kn_p}$-values (transition regime), see Rosner and Tassopoulos (1991b) and section 6.6.

values of K and $Z^{(k)}$ assembled in Table 2. If necessary, this approach could clearly be extended to other coagulation mechanisms (see, section 6, i.e. other rate constants $\beta(u, v, \ldots)$ (cf. equation (14)) appropriate to the mechanism of interest (see, e.g. Mackowski *et al.*, 1991).

3.5. *Coupled ODEs for free-molecule and continuum coagulation; steady, quasi-one-dimensional duct flow with simultaneous wall losses*

Combining the results of sections 3.1–3.4 above, we see that, subject to the assumptions of section 2, in all cases the PSD moments M_k ($k = 0, 1, 2$) will satisfy the coupled ODEs:

$$U\frac{dM_k}{dz} = -\frac{P}{A}\cdot U \cdot \mathrm{St_m}(\bar{v}) \cdot F_k M_k + \frac{1}{2}KM_0^2 Z^{(k)}, \tag{16}$$

where F_k is the above-mentioned moment shift function appropriate to the mass transfer law (section 3.3) and the appropriate values of $K(T, \ldots)$ and $Z^{(k)}$ appearing in the coagulation rate terms can be read from Table 2. All of the conclusions we derive and state below follow from these coupled non-linear ordinary differential equations and the abovementioned moment interrelations. Before proceeding it is worth noting that the coagulation term (second term on RHS) will not appear in the ODE governing $M_1 (\equiv \phi_p)$; i.e. $Z^{(0)} = 0$. Moreover, if instead of an axial position variable z measured downstream from the sampling duct inlet $z = 0$ (with $0 < z < L$) we introduce a position variable x measured upstream from the aerosol instrument at $z = L$ then $x = L - z$ and $dx = -dz$. Thus, introduction of such a variable (to form the corresponding $U(dM_k/dx)$ equations) will merely change the sign of all terms on the RHS of equation (16). This sets the stage for the 'backward' integration of equation (16) to find the upstream dependence of the aerosol PSD moments based on a knowledge (measurement) of their downstream (instrument) values.

3.6. *Non-dimensionalized inverse problem ODEs*

In Rosner and Tassopoulos (1990, 1991b) we illustrated the use of equation (16) to calculate the downstream evolution of the aerosol PSD in terms of inlet values and associated dimensionless coagulation parameters for a variety of flow conditions (laminar, turbulent, free-molecule transport, continuum transport). To solve the 'inverse' problem of aerosol sampling theory, we merely redefine our dimensionless variables and parameters using downstream values (presumed measured) and integrate in the upstream direction. Thus, we here introduce $\tilde{N} \equiv N_p/N_{p,L}$, $\tilde{\phi} \equiv \phi_p/\phi_{p,L}$, $\tilde{M}_2 \equiv M_2/M_{2,L}$ and define the 'rescaled' axial distance variable:

$$\xi \equiv \left\{\frac{P}{A}\mathrm{St_m}(\bar{v}_L) \cdot F_{o,L}\right\} \cdot (L - z). \tag{17}$$

The coupled ODEs satisfied by $\tilde{N}(\xi, \ldots)$, $\tilde{\phi}(\xi, \ldots)$ and $\tilde{M}_2(\xi, \ldots)$ can be obtained from the dimensionless ODEs of Rosner and Tassopoulos (1990, 1991) by making the appropriate parameter replacements and sign changes, with the following results. Let us introduce the coagulation parameter:

$$C \equiv \frac{(-Z_L^{(0)}) \cdot (\frac{1}{2}K) \cdot N_{p,L}^2}{\left\{\left(\frac{P}{A}\right) \cdot U \cdot \mathrm{St}_m(\bar{v}_L) \cdot F_{o,L} \cdot N_{p,L}\right\}} \tag{18}$$

(a measure of the relative importance of coagulation and wall loss in altering the PSD parameters). Then, subject to the 'initial' normalization conditions: $\tilde{N}(0) = 1$, $\tilde{\phi}(0) = 1$, $\tilde{M}_2(0) = 1$ and the assumptions of section 2, the coupled dimensionless moment equations become the non-linear first order system:

$$\frac{d\tilde{N}}{d\xi} = \left(\frac{\tilde{\phi}}{\tilde{N}}\right)^b \cdot \frac{F_0}{F_{0,L}} \cdot \tilde{N} + C\tilde{N}^2 \cdot \frac{(-Z^{(0)})}{-Z_L^{(0)}} \tag{19}$$

$$\frac{d\tilde{\phi}}{d\xi} = \left(\frac{\tilde{\phi}}{\tilde{N}}\right)^b \cdot \frac{F_1}{F_{0,L}} \cdot \tilde{\phi} \tag{20}$$

$$\frac{d\tilde{M}_2}{d\xi} = \left(\frac{\tilde{\phi}}{\tilde{N}}\right)^b \cdot \frac{F_2}{F_{0,L}} \cdot \tilde{M}_2 - C\tilde{\phi}^2 \cdot \left\{\frac{2}{\exp(\ln^2 \sigma_{g,L})} \cdot \frac{(-Z^{(0)})}{(-Z_L^{(0)})}\right\}, \tag{21}$$

where the subscript L implies evaluation of the appropriate function at $z = L$ ($x = 0$). These same equations formally hold for either the free-molecule or continuum case provided the appropriate coagulation parameters/functions are introduced according to Table 2. Similarly, subject to the assumptions indicated in section 2 and discussed in section 6, they hold for either turbulent or laminar flow in a straight duct.

3.7. *Similitude implications*

Inspection of the above-mentioned moment equations governing the present simplified model reveals that the idealizations of section 2 lead to correction factors of the functional form:

$$N_{p,o}/N_{p,L} = \mathrm{fct}_0(\xi_{max}, \sigma_{g,L}, b, C) \tag{22}$$

$$\phi_{p,o}/\phi_{p,L} = \mathrm{fct}_1(\xi_{max}, \sigma_{g,L}, b, C) \tag{23}$$

$$M_{2,o}/M_{2,L} = \mathrm{fct}_2(\xi_{max}, \sigma_{g,L}, b, C) \tag{24}$$

from which we can also calculate the interesting correction factors:

$$\sigma_{g,o}/\sigma_{g,L} = \mathrm{fct}_3(\xi_{max}, \sigma_{g,L}, b, C) \tag{25}$$

$$v_{g,o}/v_{g,L} = \mathrm{fct}_4(\xi_{max}, \sigma_{g,L}, b, C), \tag{26}$$

where relevant values of the exponent b are given in Table 1, the value of the PSD spread parameter $\sigma_{g,L}$ is presumed to be measured, ξ_{max} is the value of the 'scaled' length coordinate ξ (equation (17)) evaluated at the sampling tube inlet ($z = 0$) and C is the relevant dimensionless coagulation parameter (which is seen to scale linearly with $N_{p,L}$). In section 4 we present the results of numerical integrations of (equations (19–21)) for many combinations of physical interest to display the explicit sensitivity of the desired correction factors to macroscopic flow regime (laminar, turbulent) and the Knudsen regime of particle transport. We also present an extensive set of graphical results for the commonly encountered limiting case of negligible Brownian coagulation (i.e. $N_{p,L}$ is low enough to cause $C \ll 1$). Note that, although all of our graphs deliberately go beyond the range of ξ_{max}values where the leading term of a small-ξ Taylor series expansion is valid (see section 4.2), rather frequently ξ_{max}-values of physical interest *will* be small enough to allow the simple explicit formulae of section 4.2, thus circumventing the need for the above-mentioned graphs, or specific numerical integrations (see, e.g. the numerical examples discussed in section 5).

4. RESULTS

4.1. *'Universal' graphs for convective-diffusion wall losses without (and with) appreciable particle coagulation*

In this section we display and briefly comment upon the results of our numerical integrations of the coupled set of ODEs explicitly given by equations (19)–(21) in the text,

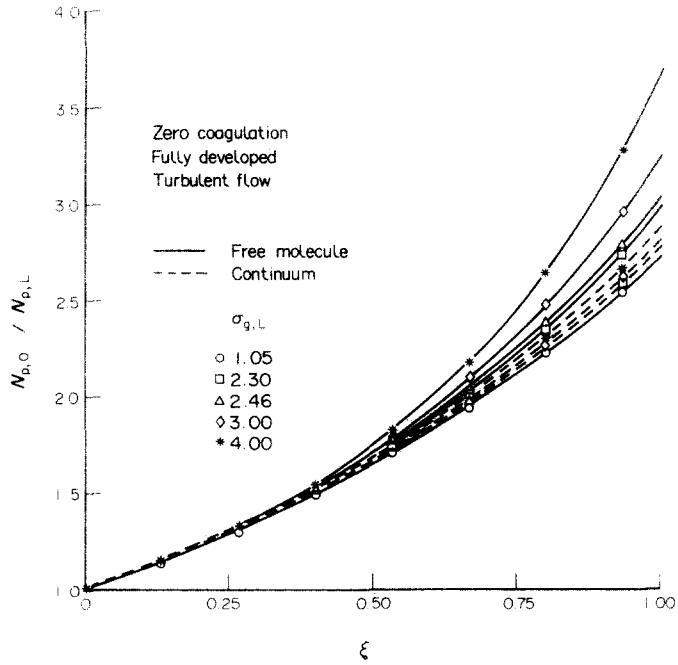

Fig. 1. Effects of particle size dependent convective-diffusion wall loss, Knudsen number regime, and PSD spread on the particle number density correction factor $N_{p,0}/N_{p,L}$ for turbulent gas flow in straight sampling tubes of scaled length ξ in the absence of appreciable Brownian coagulation.

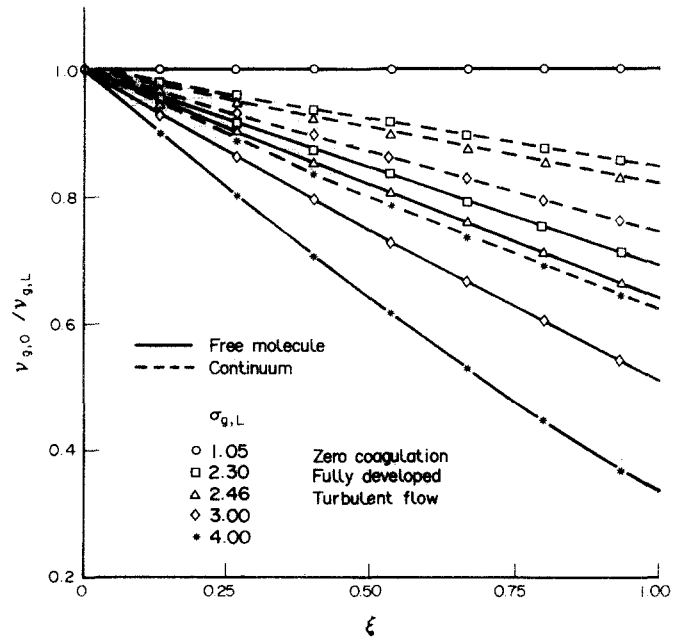

Fig. 2. Effects of particle size dependent convective-diffusion wall loss, Knudsen number regime, and PSD spread on the geometric mean particle volume correction factor $v_{g,0}/v_{g,L}$ for turbulent gas flow in straight sampling tubes of scaled length ξ in the absence of appreciable Brownian coagulation.

subject to their initial (normalization) conditions. Results are grouped as follows: Figs 1–6 pertain to PSD-parameter corrections in the limit of negligible coagulation, with the first three dealing with turbulent carrier gas flow. These graphs allow N_p-, v_g- and σ_g-corrections to be made for scaled sampling tube lengths $\xi_{max} \leq 1$ with either free-molecule or continuum

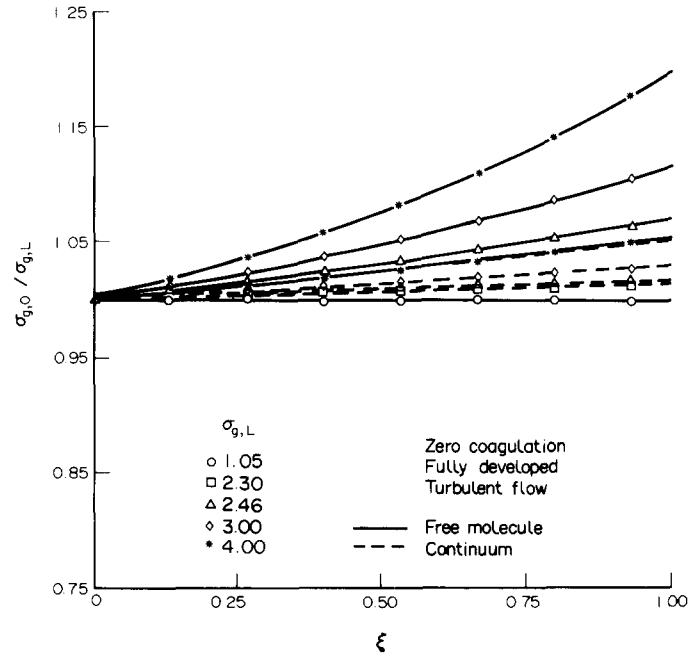

Fig. 3. Effects of particle size dependent convective-diffusion wall loss, Knudsen number regime, and PSD spread on the correction factor to the geometric PSD-spread, $\sigma_{g,0}/\sigma_{g,L}$, for turbulent gas flow in straight sampling tubes of scaled length ξ in the absence of appreciable Brownian coagulation.

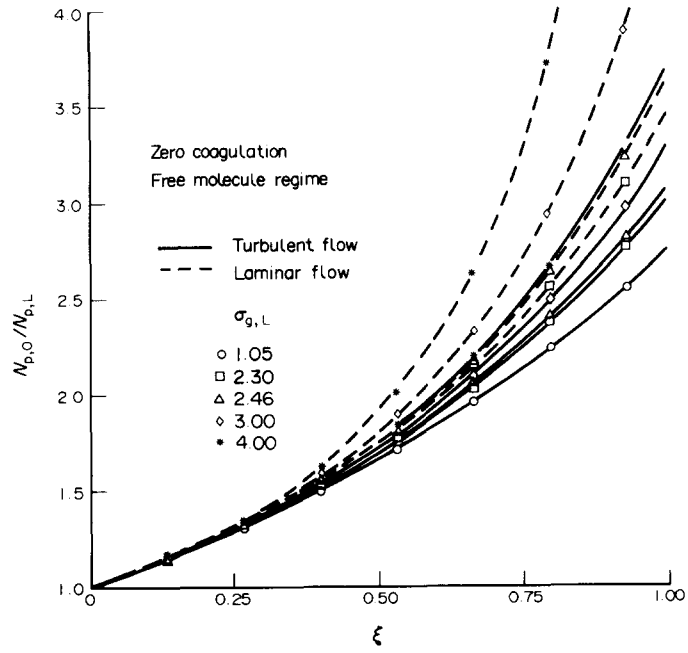

Fig. 4. Effects of particle size dependent wall loss by convective-diffusion, gas flow regime and PSD spread parameter on the total particle number density correction factor $N_{p,0}/N_{p,L}$ for gas flow in straight sampling tubes of scaled length ξ in the absence of appreciable free-molecule regime interparticle coagulation.

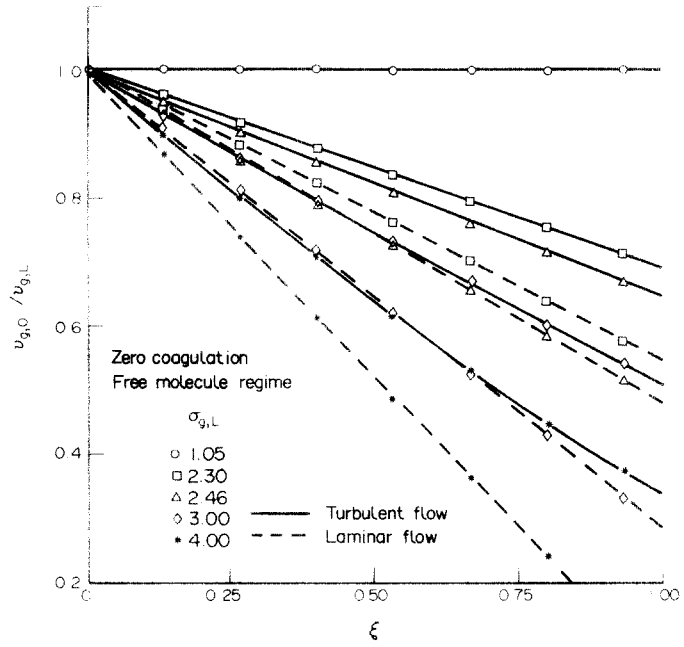

Fig. 5. Effects of particle size dependent wall loss by convective-diffusion, gas flow regime and PSD spread parameter on the geometric mean particle volume correction factor $v_{g,o}/v_{g,L}$ for gas flow in straight sampling tubes of scaled length ξ in the absence of appreciable free-molecule regime interparticle coagulation.

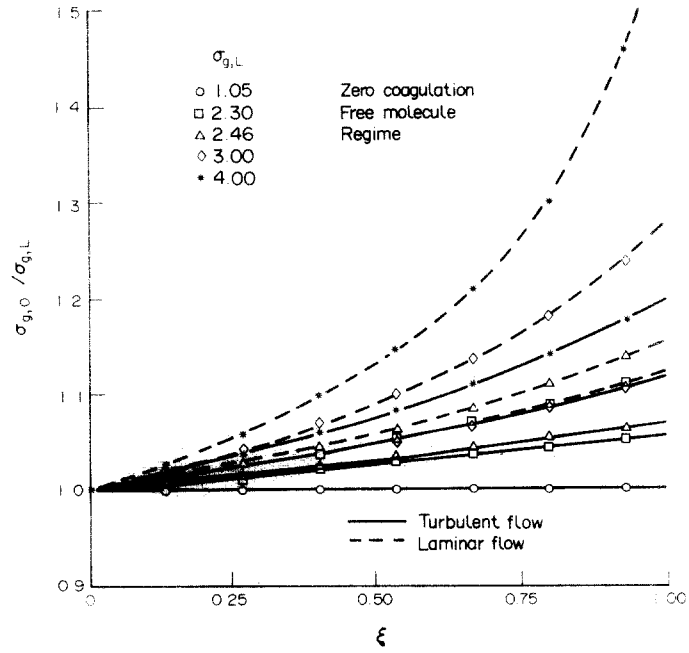

Fig. 6. Effects of particle size-dependent wall loss by convective-diffusion, gas flow regime and PSD spread parameter on the correction factor to the geometric mean PSD-spread, $\sigma_{g,o}/\sigma_{g,L}$ for gas flow in straight sampling tubes of scaled length ξ in the absence of appreciable free-molecule regime interparticle coagulation.

transport over a range of observed PSD spread parameters $\sigma_{g,L}$ at the aerosol detector. In the limit $\sigma_{g,L} \to 1$ (monodispersed) the dependence of the correction factors on Kn-regime drops out due to our choice of (scaled-) variables. For 'polydispersed' cases the correction factors are seen to depart further from unity in the free-molecule limit owing to the

increased size dependence of the Brownian diffusivity $D(v)$ when $\mathrm{Kn}_p \to \infty$. Figures 3–6 also pertain to negligible coagulation but compare laminar flow results to those for turbulent flow when the particle transport mechanism is free-molecule. As discussed in sections 5.2 and 6.1, for the laminar flow cases 'entrance effects' may dictate the need for b_{eff}-values not explicitly included in these graphs. When $\xi_{\max} < 0.5$ (say), these effects can be dealt with by using the small $\xi_{\max}$Taylor series formulae presented in section 4.2 (below) and Appendix A. For $\xi_{\max} = O(1)$ one expects $b_{\mathrm{eff}} \to b$ (Table 1) and Figs 4–6 may be useful in their present form. Note that the PSD-correction factors depart further from unity for laminar flow cases when compared at the same value of the scaled sampling system length, $\xi_{\max}$.

Figures 7–9 display our computed PSD-correction factors in the presence of appreciable interparticle Brownian coagulation effects (non-negligible C) when the gas flow is turbulent and the PSD spread parameter at the particle detector is near the appropriate 'self-preserving' value. Clearly, for any value of $\xi_{\max}$, these correction factors depart further from unity when the coagulation parameter C is increased, in either the free-molecule or continuum regimes. Particularly interesting is the rapid rise in the spread correction factor $\sigma_{g,o}/\sigma_{g,L}$ which sets in at sufficiently large $\xi_{\max}$-values (see Fig. 9). This can be shown to be a consequence of equation (3), given the sensitivity of $\tilde{N}_p$ (compared to $\tilde{\phi}_p$ and $\tilde{M}_2$) to coagulation in the sampling system.

4.2. *Small-ξ expansions*

As will be appreciated from several numerical examples (sections 5.1 and 5.2) the maximum value of ξ (the 'scaled' distance measured upstream from the aerosol instrument to the sampling tube inlet) is frequently a small number, often less than 10^{-1}. This suggests that even the above-mentioned universal graphs or the numerical integrations on which they are based can be bypassed by using a small ξ Taylor series expansion, the first terms of which can be written down by inspection of equations (20, 21). Thus, if we write:

$$\tilde{M}_k = 1 + C_1^{(k)}(C, \sigma_{g,L}, b)\xi + \text{h.o.t.} \tag{27}$$

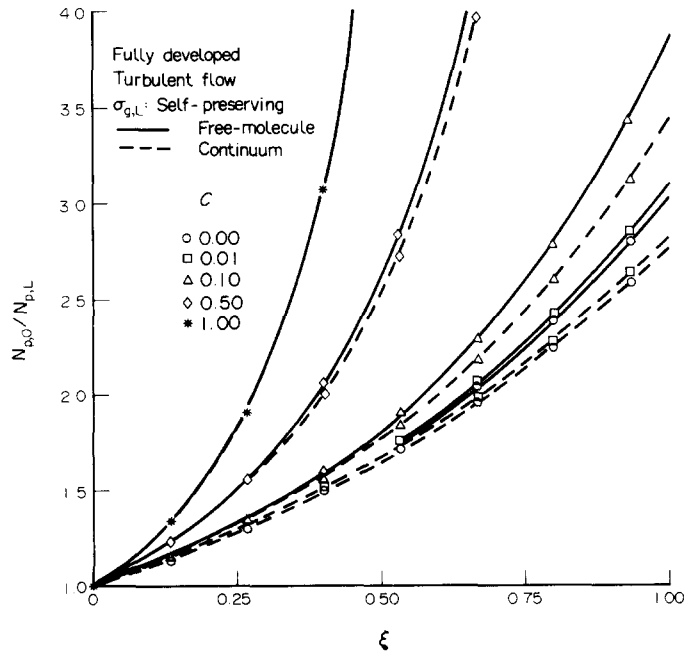

Fig. 7. Effects of Brownian coagulation, particle size-dependent convective-diffusion wall loss and particle/gas Knudsen number regime on the correction factor for total particle number density $N_{p,o}/N_{p,L}$ for turbulent gas flow in straight sampling tubes of scaled length ξ. Curves shown pertain to nearly self-preserving PSDs at the detector (i.e. $(\sigma_{g,L})_{fm} = 2.46$ and $(\sigma_{g,L})_c = 2.3$).

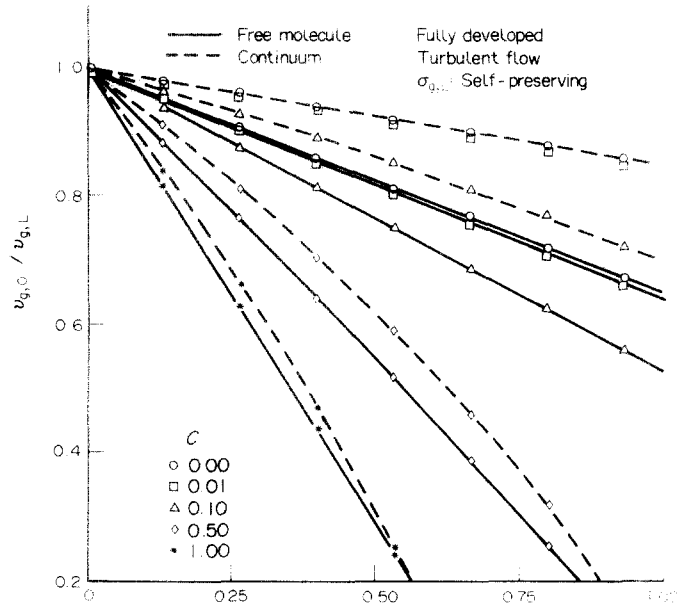

Figure 8. Effects of Brownian coagulation, particle size-dependent wall convective-diffusion loss and particle/gas Knudsen number regime on the correction factor to geometric mean particle volume $v_{g,o}/v_{g,L}$, for turbulent gas flow in straight sampling tubes of scaled length ξ. Curves shown pertain to nearly self-preserving PSDs at the detector (i.e. $(\sigma_{g,L})_{fm} = 2.46$ and $(\sigma_{g,L})_c = 2.3$).

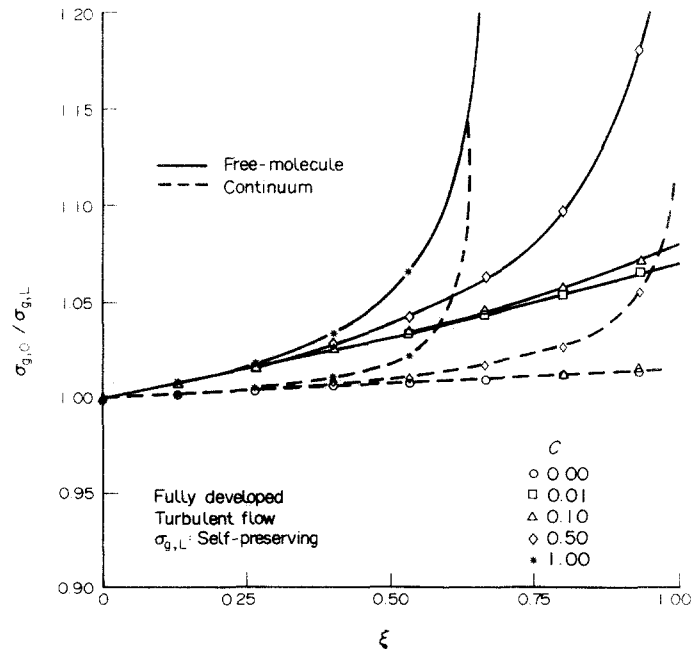

Fig. 9. Effects of Brownian coagulation, particle size-dependent wall convective-diffusion loss and particle/gas Knudsen number regime on the correction factor for to the PSD spread, $\sigma_{g,o}/\sigma_{g,L}$. Curves shown pertain to nearly self-preserving PSDs at the detector (i.e. $(\sigma_{g,L})_{fm} = 2.46$ and $(\sigma_{g,L})_c = 2.3$).

we find that the first-order coefficients† $C_1^{(k)}$ are explicitly:

$$C_1^{(0)} = 1 + C \qquad (k = 0)$$
$$C_1^{(1)} = 1 \qquad (k = 1) \tag{28}$$

and

$$C_1^{(2)} = \exp(-2b \ln^2 \sigma_{g,L}) - 2C \exp(-\ln^2 \sigma_{g,L}) \qquad (k = 2).$$

Under circumstances for which assumptions A1–6 are reasonable and the 'higher order terms' of equation (27) can be neglected† we can therefore state the following potentially useful rational explicit correction factor-relations:

$$\frac{N_{p,0}}{N_{p,L}} \cong 1 + (1 + C)\,\xi_{max} \qquad \text{(number density)} \tag{29}$$

(independent of b and $\sigma_{g,L}$)

$$\frac{\sigma_{g,0}}{\sigma_{g,L}} \approx 1 + \frac{(C_1^{(2)} + C_1^{(0)} - 2C_1^{(1)})\,\xi_{max}}{2 \ln \sigma_{g,L}} \qquad \text{(spread)} \tag{30}$$

and, since $\bar{v} \equiv (\phi_p / N_p)$ we find:

$$\frac{\bar{v}_0}{\bar{v}_L} \cong 1 - C\,\xi_{max} \qquad \text{(mean size).} \tag{31}$$

The last two equations, when combined with equation (5), immediately yield the corresponding correction to the geometric mean particle size: $v_{g,0}/v_{g,L}$,

i.e.
$$\frac{v_{g,0}}{v_{g,L}} \cong 1 - [C + \tfrac{1}{2}(C_1^{(2)} + C_1^{(0)} + C_1^{(1)})]\,\xi_{max}. \tag{32}$$

Thus, it would appear that when $\xi_{max} \lesssim 0.3$ (say) and the assumptions A1–7 are simultaneously reasonable equations (29)–(31) can provide acceptable rational corrections to measured aerosol data to account for the systematic effects of upstream coagulation and/or wall losses. It is interesting to note that while in the explicit forms stated they appear to be valid for either‡ laminar or turbulent gas flow, and free-molecule or continuum particle transport, in practice they would often incur unacceptably large errors for laminar flow systems due to so-called 'entrance'-effects on the mass transfer coefficient (see, e.g. sections 5.2 and 6.1, and Rosner (1986)). A numerical procedure to effectively eliminate such errors without introducing any new parameters has been developed (Rosner and Tassopoulos, 1991b) but is beyond the scope of the present paper. However, the present results can be approximately corrected for this effect by simply replacing the 'fully-developed' value of $\mathrm{St}_m(\bar{v}_L)$ $(= \mathrm{Nu}_m/(\mathrm{ReSc}))$ by the streamwise-integrated average value $\bar{F}$(entrance)$\cdot \mathrm{Nu}_m$(fully developed)$/(\mathrm{Re} \cdot \mathrm{Sc}(\bar{v}_L))$ and by introducing an effective value of the St_m-exponent b, written b_{eff}, which varies between $-4/9$ and $-2/3$ (Table 1) according to the value of $\bar{F}$(entrance). This correction procedure for the present laminar results, using Nu_m(fully developed) $= 3.657$ for a straight circular duct, is illustrated in section 5.2.

4.3. *Direct numerical integration for particular cases*

The 'universality' of the results derived and presented above, and the relatively small number of dimensionless parameters on which they depend (section 3.7), of course follow from our underlying idealizations, made explicit in section 2. However, the basic moment-method approach (section 3), together with our treatment of wall losses (section 3.3) and

† Closed-form expressions are available for the $C_2^{(k)}$ coefficients (of ξ^2) (see Appendix A).

‡ These physical differences do, of course, affect the results, but only implicitly via establishment of the appropriate values of ξ_{max}(equation (3.6–1)) and the St_m exponent b (see Table 1).

interparticle coagulation (section 4, and the primary references cited therein) can clearly be used to obtain PSD-parameter correction factors in much more complicated aerosol sampling duct situations, such as for example, systems which are cooled near the inlet (to prevent thermal failure) and subsequently heated (to prevent water vapour condensation) for extracting carbonaceous soot (smoke) aerosols from gas turbine engine combustors (see, e.g. Colket *et al.* (1977), and section 6). In such cases the recommended procedure would be to integrate the appropriate coupled set of ODEs (of the form of equation (16), but with the LHS written $\{(1/A)\mathrm{d}(AUM_k)/\mathrm{d}z\}$ and introduction of the 'upstream' position variable $x = L - z$), after incorporating the required special features of the sampling system of particular interest (see sections 6.1–6.12).

5. IMPLICATIONS AND APPLICATIONS

To fix ideas, become familiar with typical orders-of-magnitude, and illustrate how to use the results calculated/presented in section 4 it is useful to briefly consider at least two specific numerical examples that arise in conveying aerosol samples to a 'remote' instrument via a constant area duct. The first (section 5.1) is based on an exercise in Friedlander's 1977 textbook involving turbulent gas flow in a ground-based aerosol sampling system. The second example involving laminar gas flow is based on conditions encountered in a proposed system for sampling the Earth's atmosphere from a research aircraft flying at ca. 8 km altitude. In both cases we examine log-normal distributions of highly submicron particles for which wall losses are often non-negligible even for relatively 'short' ducts. We also define the total concentration levels beyond which Brownian coagulation processes of such particles within the duct will become non-negligible. Explicit applications to more complex (e.g. diabatic) systems, as frequently encountered in sampling combustion engines, are beyond the scope of this paper (see sections 4.3 and 6).

5.1. *Turbulent flow in duct of ground-based air monitoring station*

Exercise 5, Chapter 3 of Friedlander (1977) deals with a ground-based air monitoring station. Outside air is delivered to the aerosol instruments via a 2-in diameter, 12-ft long duct at a mean velocity of 10 ft s^{-1}. The goal is to "calculate the correction factor that must be applied for submicron particles as a result of diffusion to the walls of the duct, e.g. the percentage by which the measured concentration must be altered to provide the true (ambient) concentration as a function of particle size". To illustrate our procedures let us imagine that the aerosol instrument 'sees' a sub-micron aerosol PSD which is log-normal with a spread of $\sigma_g = 2.46$ and a geometric mean diameter corresponding to $\bar{d}_p = 0.02\ \mu$m, i.e.:

$$d_g = \bar{d}_p \cdot \exp[-\tfrac{1}{6}\ln^2 \sigma_g] = (0.02\ \mu\mathrm{m}) \cdot \exp[-\tfrac{1}{6}\ln^2(2.46)] = 0.0175\ \mu\mathrm{m}. \tag{33}$$

The Brownian diffusivity D_p for a 0.02 μm diameter particle in, say, 20°C air at 1 atm is (see, e.g. Table 2.1, Friedlander (1977)) 1.34×10^{-4} $\mathrm{cm^2\,s^{-1}}$ and (since the momentum diffusivity of air is 1.50×10^{-1} $\mathrm{cm^2\,s^{-1}}$ under these same conditions) we also find that $\mathrm{Sc}(\bar{v}_{p,L}) \equiv \nu/D_p(v_{p,L}) = 1.12 \times 10^3$ for the mean particle diameter. The mass transfer coefficient $\mathrm{St_m}$ appropriate to this case can be estimated once the Reynolds number Ud_w/ν characterizing this air flow is determined. Converting to metric units we find that $d_w = 5.08$ cm, $U = 3.05 \times 10^2$ cm s^{-1} and, therefore, $\mathrm{Re} = 1.03 \times 10^4$, which is well into the turbulent range. For a smooth wall straight duct and particles in this size range (see section 6.7) $\mathrm{St_m}$ can therefore be estimated from, say, equation (6.5–11b) of Rosner (1986), i.e.:

$$\mathrm{St_m} \approx 0.0889\left(\frac{C_f}{2}\right)^{1/2} \cdot \mathrm{Sc}^{-0.704} \qquad (\mathrm{Sc} \gg 1), \tag{34}$$

where $C_f(\mathrm{Re})$ is the friction factor (non-dimensional time-averaged shear stress at the hydraulically smooth duct wall) corresponding to the prevailing Reynolds number. This can be estimated as $0.079\ \mathrm{Re}^{-1/4}$ so that $C_f = 0.783 \times 10^{-2}$, $(C_f/2)^{1/2} = 0.626 \times 10^{-1}$ and, hence,

$St_m(\bar{v}_{p,L}) \approx 3.97 \times 10^{-6}$ (via equation (34)). We are now in a position to calculate the decisive dimensionless 'scaled' length of the sampling tube, i.e.:

$$\xi_{max} \equiv 4\left(\frac{L}{d_w}\right) \cdot \mathrm{St}_m(\bar{v}_{p,L}) \cdot F_{0,L} \tag{35}$$

$$\xi_{max} \equiv 4\left(\frac{L}{d_w}\right) \cdot \mathrm{St}_m(\bar{v}_{p,L}) \cdot \exp\left[\frac{b(b-1)}{2} \cdot \ln^2 \sigma_{g,L}\right] = 1.51 \times 10^{-3},$$

where we have used the fact that $L = 3.66 \times 10^2$ cm, $L/d_w = 72$ and (see Table 1) $b \cong -0.469$ for particles which are small compared to the prevailing gas-free-path (0.065 μm). In this case, since ξ_{max} is small, the Taylor series results of section 4.3 will be useful, i.e.:

$$\frac{N_{p,0}}{N_{p,L}} \cong 1 + (1 + C_{fm})\,\xi_{max}, \tag{36}$$

so that if coagulation is negligible (i.e. $C_{fm} \ll 1$ (see below)) then $N_{p,0}/N_{p,L} = 1 + 1.51 \times 10^{-3} = 1.0015$. Thus, under such conditions total number densities in the ambient atmosphere would only be about 0.15% above those present at the detector. Based on the definition of the dimensionless coagulation parameter C_{fm} it is also possible to calculate the level of particle number density, $N_{p,L}$ at which coagulation effects and wall loss effects on $N_{p,o}/N_{p,L}$ would be comparable—i.e. conditions corresponding to $C_{fm} = 1$. In the present case:

$$C_{fm} \equiv \frac{(-Z^{(0)}_{fm,L})(\frac{1}{2}K_{fm})N_{p,L}}{4/d_w \cdot U \cdot \mathrm{St}_m(\bar{v}_{p,L}) \cdot F_{0,L}}. \tag{37}$$

Setting $C_{fm} = 1$ and evaluating the factors $(-Z^{(0)}_{fm,L})$ and $\frac{1}{2}K_{fm}$ from their respective definitions (see Table 2, first row) we find that $C_{fm} = 1$ when $N_{p,L} \cong O(1.1 \times 10^7$ particles $\mathrm{cm}^{-3})$, a level that could be experienced near pollutant sources. However, on the assumption that particle concentrations are frequently much lower than this we proceed to calculate the (small) corrections needed to arrive at the ambient PSD parameters $\sigma_{g,o}$ and $v_{g,o}$. These can be obtained from equations (30) and (32), respectively. In this case: $C_1^{(0)} = 1$, $C_1^{(1)} = 1$, $C_1^{(2)} = \exp[-2(-0.469)\ln^2(2.46)] = 2.138$ so that:

$$\frac{\sigma_{g,0}}{\sigma_{g,L}} \approx 1 + \frac{(2.138-1)(1.51 \times 10^{-3})}{2\ln(2.46)} = 1.00095$$

and:

$$\frac{(d_{p,g})_0}{(d_{p,g})_L} \approx \exp(-\tfrac{1}{6}(2.138-1)(1.51 \times 10^{-3})) = 0.9997,$$

i.e. when $\bar{d}_{p,L} = 0.02$ μm and $\sigma_{g,L} = 2.46$ the systematic corrections are modest indeed. However, the present formulation has the merit that it allows rapid calculations of corrections under other conditions of $d_{p,L}$, $\sigma_{g,L}$, L/d_w, U, . . . for which the corresponding corrections due to wall loss and/or coagulation may be appreciable, including cases requiring the graphs of sections 4.1 and 4.2 rather than the small ξ_{max}expansions of section 4.3 and Appendix A.

5.2. *Laminar flow in sampling tube upstream of an airborne condensation nucleus counter*

As our second specific example consider the following set of conditions typical of an airborne condensation nucleus particle counter (CNC) system for flight at an altitude of 25,000 ft. Suppose the cabin instrument package sees an aerosol with a mean particle diameter $\bar{d}_{p,L} \cong 0.014$ μm and a spread parameter of 2.46 in air at a volume flow rate of 24 $\mathrm{cm}^3\,\mathrm{s}^{-1}$, with the pressure and temperature levels established at 0.4 atm and 244 K,

respectively. If the insulated upstream tube that conveys the aerosol sample to the instrument has a length of 121 cm and an internal diameter of 0.953 cm then we seek to estimate the correction factors $N_{p,o}/N_{p,L}$, $\sigma_{g,o}/\sigma_{g,L}$ and $d_{g,o}/d_{g,L}$ to be applied to data recorded at the instrument in order to estimate the corresponding aerosol properties in the local troposphere.

If we tentatively assumed 'fully-developed' particle mass transfer in this $L/d_w = 128$ sampling tube system (see, however, section 6.1 and below) we would proceed as follows: Under the stated conditions the Reynolds number Ud_w/ν can be calculated to be only 1.165×10^2 so the gas flow will be *laminar*. The prevailing mean-free-path under the above-mentioned conditions is about 0.2 μm so that $\mathrm{Kn_p}(\bar{v}_{p,L}) = 14.4$ and most particles will experience conditions appropriate to free-molecule (fm) flow. In particular, the mean size particle will be characterized by a Brownian diffusivity of about 0.93×10^{-3} cm^2 s^{-1}, corresponding to a Schmidt number $\mathrm{Sc} = \nu/D_p$ of about 2.96×10^2. For fully-developed steady laminar flow in a straight circular duct it is well known that $\mathrm{Nu_m} = 3.657$ (Nusselt) so that:

$$\mathrm{St_m}(\bar{v}_L) = \frac{\mathrm{Nu_m}}{\mathrm{Re}\cdot\mathrm{Sc}} = \frac{3.657}{(1.165\times 10^2)(2.96\times 10^2)} = 1.06\times 10^{-4}. \tag{38}$$

It would follow that:

$$\xi_{max} = 4\left(\frac{L}{d_w}\right)\cdot \mathrm{St_m}(\bar{v}_L)\cdot \exp\left[\frac{b(b-1)}{2}\ln^2\sigma_g\right] = 0.852\times 10^{-1} \tag{39}$$

since (Table 1) $b = -2/3$. If the coagulation parameter $C_{fm} \ll 1$ (see below) then this would correspond to $N_{p,o}/N_{p,L} \cong 1.085$ due to particle size-dependent wall loss (based, again, on equation (29)). Noting that $C_1^{(2)} = \exp\{-2(-2/3)\ln^2(2.46)\} = 2.947$ we find (equation (30)) that the remaining correction factors are: $\sigma_{g,o}/\sigma_{g,L} \approx 1.09$ and $d_{g,o}/d_{g,L} \approx 0.973$ (equation (32)). Returning to the possibility of coagulation effects, we can calculate what particle number density $N_{p,L}$ would be required to cause $C_{fm} \approx 10^{-1}$, say. Since this turns out to be *ca* 3×10^6 cm^{-3} in the present case (a value very far in excess of ambient atmosphere particle number densities (O(10^{-2} cm^{-3}) at such altitudes) the neglect of coagulation in such sampling tubes is seen to be self-consistent.

Returning to the question of the validity of our tentative assumption of 'fully-developed' particle mass transfer (i.e. A4, negligible 'entrance effect') we note that while the viscous flow itself would become fully-developed (z/d_w-independent) beyond a L/d_w of only about $0.2\mathrm{Re} = 23$, the value of $\mathrm{St_m}$ will not approach the fully-developed asymptote until L/d_w is about $0.2\mathrm{ReSc} = 6900$. Since the actual L/d_w of the system is 128 we see *a posteriori* that A4 is not justified under such laminar flow conditions (see section 6.1). All is not lost, however, since there is good reason to believe that if ξ_{max} is recalculated using the actual length-averaged transfer coefficient, and an effective value of b appropriate to the magnitude of the entrance effect, then our previous formulas (or graphs) will provide a useful first approximation. The 'entrance-effect' correction factor $\bar{F}_e$ to the fully-developed value of $\overline{\mathrm{Nu}}_m$ or $\overline{\mathrm{St}}_m$ is known to depend upon the dimensionless distance variable:

$$\frac{1}{\mathrm{Re}\cdot\mathrm{Sc}}\cdot\frac{L}{d_w} \equiv \zeta_m(\text{say}). \tag{40}$$

For fully-developed laminar flow in a straight circular duct a convenient approximation to $\bar{F}$(entrance) is (see, e.g. Rosner, 1986)

$$\bar{F}_e \approx [1+(7.60\zeta_m)^{-8/3}]^{1/8}, \tag{41}$$

which, in the present case, gives $\bar{F}_e = 3.29$ corresponding to $\overline{\mathrm{St}}_m(\bar{v}_L) = 3.49\times 10^{-4}$. Using the appropriate "effective" value of b obtained from

$$b_{eff} = -\frac{2}{3}\cdot\left[1+\frac{d\ln\bar{F}_e}{d\ln\zeta_m}\right] \cong -\frac{2}{3}\left[1-\frac{1}{3}(1-\bar{F}_e^{-8})\right] \approx -\frac{4}{9} \tag{42}$$

(see, e.g. Rosner and Tassopoulos, 1991) we then recalculate the values of ξ_{max}, this time obtaining $\xi_{max}= 0.30$, corresponding to $N_{p,o}/N_{p,L} \cong 1.3$. Recomputing the remaining correction factors now gives $\sigma_{g,o}/\sigma_{g,L} \cong 1.18$ and $d_{g,o}/d_{g,L} \approx 0.95$. Based on the present work this would provide the best current estimate of the required correction factors in this laminar flow aerosol sampling system. More rigorous calculations (now underway) will be necessary to test the accuracy of this plausible, proposed correction procedure (for relaxing A4).

In the light of these two simple numerical examples, both involving highly submicron, dense (*ca* $\tilde{\rho}_p = 1.83\ \mathrm{g\,cm^{-3}}$) spherical particles in straight nearly adiabatic sampling ducts but one with laminar flow (section 5.2) and one with turbulent flow (section 5.1), it is now appropriate to briefly discuss many of the abovementioned assumptions, indicating, where possible, methods to generalize the treatment to include less 'idealized' cases often encountered in sampling from industrially important devices (e.g. combustors for propulsion or power generation).

6. DISCUSSION OF ASSUMPTIONS AND GENERALIZATIONS

It is prudent to consider the domain of validity of the underlying assumptions of section 2 and useful to indicate here how readily some of these assumptions can be relaxed, thereby opening the door to the quantitative treatment of much more complex sampling duct situations.

6.1. *Entry effects*

Even apart from development of the viscous gas flow itself, the mass transfer boundary layers within the sampling tube require a 'development length' before $\mathrm{St_m}$ (equation (6)) becomes essentially independent of z/d_w. For laminar mass transfer boundary layers the required number of duct diameters is approximately:

$$\left(\frac{L}{d_w}\right)_{req} = 0.2(\mathrm{Re}\cdot\mathrm{Sc}), \tag{43}$$

which, for the example of section 5.2, is about 6900, far in excess of the actual L/d_w of the sampling system (128) or the L/d_w required for development of the host gas flow itself (*ca* 23). Thus, unless much smaller particles are of interest, Assumption 4 will *not* be defensible for many *laminar* flow sampling systems. A rational 'correction' for this can, however, be made when coagulation is negligible (using the actual length-averaged $\overline{\mathrm{St}}_m$-value in the definition of ξ and modifying the effective exponent b, as discussed in section 5.2) or specific results can be generated for laminar sampling systems by accurately including such mass transfer 'entrance effects' (Rosner and Tassopoulos, 1991a). For *turbulent*, high Sc systems the situation is much improved and $(L/d_w)_{req}$ will ordinarily be less than about 30, a condition which is frequently met*, and certainly met in the ground-based air monitoring application discussed in section 5.1.

6.2. *Variable* $\mathrm{d_{eff}} \equiv 4\mathrm{A(z)/P(z)}$

If the effective duct diameter d_{eff} is not constant, but sufficiently slowly varying, then the quasi-one-dimensional equations (equation (16)) remain valid, and such geometric effects can clearly be incorporated in the numerical integrations. In many situations d_{eff} will be piecewise-constant, in which case our analysis would apply to each *segment* of the system but with the effective lengths of the segments modified to allow for the inevitable 'entrance-effects' near each juncture (see, e.g. section 6.1).

* Colket *et al.* (1977) describe a diabatic system with $L/d_w \approx 2200$ for sampling from gas turbine combustors.

6.3. *Bends*

Because of the secondary flows and turbulence modulation associated with bends in a "piecewise straight" sampling system $St_m(z/d_w, Re, Sc)$ will be modified in accord with the curvature d_w/R and included angle of the bend. Recent (vapor) mass transfer data of this type (see, e.g. Sparrow and Chrysler (1986) and Ohadi and Sparrow (1989, 1990)) are now being mobilized and recast so that it may be conveniently used in the present type of quasi-one dimensional, $Sc \gg 1$ analysis (Rosner *et al.*, 1991).

6.4. *Heated (cooled) ducts*

Inadvertent or deliberate heat transfer can dramatically alter the rates of fine particle loss to the wall, and the particle size-dependence of this rate (cf. the St_m exponent b) as a result of particle thermophoresis. The laws of particle thermophoresis (drift down the transverse temperature gradient) have been under extensive development in the last 15 years (see, e.g. the recent review of Rosner *et al.*, 1990) and it has been shown that for submicron particles deliberately heated ducts can be used to sharply reduce wall deposition rates [see, e.g. Gokoglu and Rosner (1986) (before the gas temperature 'catches up' with the wall temperature]. While beyond the scope of the present paper, it can be shown that in some cases (e.g. constant wall heat flux (addition)) the present results can be used as a first approximation with a suitably reduced St_m-value and a modified (more negative) b_{eff}-value (Rosner and Tassopoulos, 1991b). In some cases wall cooling may be necessary near the inlet to prevent local probe failure (as in extracting samples from high temperature combustors (Colket *et al.* (1977), arcjets, etc.). This can cause appreciable local particle losses to the wall unless the wall cooling is accomplished by foreign gas transpiration (see, e.g. Gokoglu and Rosner, 1985). Sometimes downstream heating is also used to prevent the condensation of a co-present vapor, as in sampling the combustion products of a gas turbine combustor.

6.5. *Single mode log-normality*

Aerosols formed from several distinct mechanisms may exhibit a multi-modal PSD, each mode of which can be represented by a log-normal distribution. If (as is often the case) further coagulation can be neglected within the aerosol sampling tube then our present results can be applied without modification to each mode. In the presence of appreciable coagulation this is no longer possible and results would have to be obtained using an extended coagulation rate theory along the lines of Megaridis and Dobbins (1990a) to deal with particular cases of interest.

6.6. Kn_p-*interpolation*

If an appreciable portion of the aerosol is in the transition regime of $Kn_p = O(1)$, then neither of the above-mentioned asymptotic regime results ($Kn_p \gg 1$ called free-molecule, or $Kn_p \ll 1$ called continuum) would provide an accurate description. This influences both the wall loss behavior (via its effect on the Brownian diffusion law $D(v)$) and the coagulation rate behavior (via the collision rate constant β, which will differ from either of the previously considered asymptotes β_{fm} and β_c). A general treatment of this regime is possible, which will introduce an additional parameter like the Knudsen number based on the median diameter $(6v_{g,L}/\pi)^{1/3}$. In the absence of coagulation the principal effects are to modify $St_m(\bar{v}_L)$ and the effective values of the St_m-exponent b. In the presence of coagulation, use can be made of the simple and successful so-called 'harmonic-average' approximation for the coagulation rate constant, i.e. $\beta^{-1} \approx \beta_{fm}^{-1} + \beta_c^{-1}$ which can be introduced to generalize the moment-method treatment of section 3.4 (Rosner and Tassopoulos, 1991b) (for an alternative but closely related approach, see Pratsinis and Kim (1989) and Biswas *et al.* (1989)).

6.7. *Eddy-impaction*

When the sampling duct flow is turbulent ($Re > 2.3 \times 10^3$, say) and a significant portion of the aerosol is associated with dimensionless particle stopping times $t_p^+ (\equiv u_*^2 t_p/\nu)$ greater than about $16.5\,(Sc)^{-0.352}$ then time-averaged wall losses will be enhanced by the mechanism of 'eddy-impaction' (see, e.g. the brief summary of available correlations contained in Rosner and Tassopoulos (1989)), which also modifies the effective value of the exponent b for that portion of the aerosol. Only when eddy-impaction is the dominant mechanism and $St_m \sim (t_p^+)^2$ for most of the prevailing particles can our present formulation be retained, but with $b = +1.333$ (see Rosner and Tassopoulos, (1989)). However, for the illustrative problem discussed in section 5.1 we find that eddy-impaction would not set in until $d_p = 3.8\ \mu m$, a size beyond which there are few particles indeed. Thus, the previous treatment is self-consistent in this respect. Other effects associated with the mass of the suspended particles (e.g. sedimentation and/or inertial impaction in bends) are likewise expected to be negligible.

6.8. *Turbulent coagulation*

In principle, new mechanisms of suspended particle–particle coagulation/coalescence occur in turbulent flows (Friedlander, 1977) which could be incorporated within our moment method calculation of coagulation via the appropriate $\beta(u, v, \ldots)$ functions. However, even in turbulent flows sufficiently small suspended particles (the ones likely to be numerous enough) will still coagulate according to the Brownian laws discussed in section 2, especially in initially well-mixed (homogeneous) submicron aerosol situations at the inlet. In many cases even such small particles may not be numerous enough to warrant the inclusion of coagulation within the sampling tube (see the examples of sections 5.1 and 5.2).

6.9. *Axial dispersion*

For radially nonuniform velocity steady flow in a duct the effective axial diffusivity is known to be larger than the true Brownian diffusivity by the Taylor-contribution (see, e.g. Butt, 1980; Denbigh and Turner, 1971; Probstein, 1989)

$$(D_{eff})_{Taylor} = \begin{cases} \dfrac{Re \cdot Sc}{192} \cdot U d_w & \text{(laminar)} \\ 5\left(\dfrac{C_f}{2}\right)^{1/2} \cdot U d_w & \text{(turbulent)} \end{cases} \tag{44}$$

so that Assumption 3 (section 2) is equivalent to satisfying the inequality:

$$\left(\frac{D_{eff}}{UL}\right) \cdot \left(\frac{N_{p,0}}{N_{p,L}} - 1\right) \ll 1. \tag{45}$$

This criterion is readily satisfied in the turbulent flow example (section 5.1) but is only marginally satisfied in the laminar flow example (section 5.2). In both examples the effective axial diffusivity in completely dominated by the fluid-dynamic (Taylor) contribution. These results again suggest (cf. section 6.1) that the idealizations exploited in the present work are more appropriate to turbulent flow sampling systems (section 5.1) than laminar flow sampling systems (section 5.2), and that many laminar systems will warrant a more accurate treatment than that indicated in section 5.2, even including the above-mentioned 'entrance-effect' correction (section 6.1).

6.10. *Aggregate deposition/coagulation*

For non-coalesced aggregates comprised of primary particles of volume v_1 each depositing 'particle' will have the total volume $v = nv_1$, where n is some integer (see, e.g. Megaridis

and Dobbins, 1990b). Such aggregated particles will have orientation-averaged Brownian diffusivities which will depend not only upon v but also on the particular morphology (arrangement of the primary particles). In each case we can write:

$$b \equiv \frac{\partial \ln \mathrm{St}_m}{\partial \ln v} = -\frac{\partial \ln \mathrm{St}_m}{\partial \ln \mathrm{Sc}} \cdot \left(\frac{\partial \ln D}{\partial \ln v} \right). \tag{46}$$

Thus, when coagulation is negligible, a knowledge of $\mathrm{St}_m(v)$, where $v = nv_1$ and of the appropriate value of $\partial \ln D / \partial \ln v$ for the morphology is question will also allow useful predictions to be made for aggregated particles (see, e.g. Rosner, 1991; Rosner *et al.*, 1991). A treatment of suspended aggregate–aggregate coagulation analogous to that outlined in section 3.4 is apparently not yet available.

6.11. *Non-power law capture*

If the Schmidt number dependence of St_m deviates from a simple power law and/or $D(v)$ departs from a simple power-law then the value of the exponent b will not be a constant (cf. equation (46)) and corrections to the convenient computational procedures exploited here will be necessary. In Rosner (1989) we showed that these corrections depend upon $(\partial^2 \ln \mathrm{St}_m / \partial \ln^2 v)_{\bar{v}}$ and the local spread of the PSD. This provides either a testable criterion for the validity of power-law behavior in any particular case or the basis of a systematic correction procedure for the calculation of the factor F_k (cf. equation (12)) (see, e.g. Rosner and Tassopoulous (1991b)). For straight duct high Schmidt number turbulent convective-diffusion transport in either the free-molecule (fm) or continuum (c) limits these corrections vanish and the exponents (b-values) presented in the second row of Table 1 are true constants. However, it should be realized that no single mechanism of particle transport (hence $\mathrm{St}_m(v)$-law) is strictly valid over the entire range of particle sizes (see, e.g. Rosner and Tassopolous, 1989). Furthermore, even when a single deposition mechanism dominates, departures from simple power-law behavior may be associated with fluid-dynamic non-idealities, such as developing-(section 6.1) and/or secondary-flows (cf. section 6.3)

6.12. *Vapor growth/particle evaporation*

In the present analysis we assumed that the suspended particles are stable with respect to evaporation or growth by vapor condensation in the prevailing carrier gas environment (A7). In "diabatic" sampling tube cases (often encountered in extractive sampling from hostile environments, such as gas turbine engine combustors) this may not be valid and the analysis of section 3 would then have to be generalized by including the contribution to the $U\mathrm{d}M_k/\mathrm{d}z$ due to vapor growth (see, e.g. Friedlander, 1977; Megaridis, 1987; Megaridis and Dobbins, 1989) coupled with balance equations for the vapor concentration and the bulk (mixing cup-averaged) gas temperature. The present class of moment methods would also make specific calculations of this type feasible, however, the assumption of log-normality could prove overly restrictive in many such instances (see, e.g. Landgrebe and Pratsinis, 1989; Landgrebe, 1989; Biswas *et al.*, 1987; Mackowski *et al.*, 1991).

7. CONCLUSIONS, RECOMMENDATIONS AND FUTURE WORK

A simple, rational, moment-based method is presented for correcting aerosol sampling data for the systematic upstream effects of particle size-dependent wall losses and, if necessary, particle–particle coagulation. 'Universal' graphs and rational formulae are developed and provided for the commonly encountered cases of log-normally distributed aerosols in straight adiabatic ducts of constant cross-section/'wetted' perimeter for the limiting cases of free-molecule particle transport ($\mathrm{Kn}_p \gg 1$) and continuum particle transport ($\mathrm{Kn}_p \ll 1$). In many cases the leading terms of a Taylor series expansion in the dimensionless distance (proportional to $(L/d_w)\mathrm{St}_m(\bar{v})$) will be adequate to provide the

desired correction factors: $N_{p,o}/N_{p,meas}$, $\phi_{p,o}/\phi_{p,meas}$ and $M_{2,o}/M_{2,meas}$ as well as $v_{g,o}/v_{g,meas}$ and $\sigma_{g,o}/\sigma_{g,meas}$. In more general cases backward numerical integration of the relevant coupled moment equations is recommended, allowing several of the idealizations discussed in sections 2 and 6 to be simultaneously relaxed. In addition to providing a simple yet rational basis for correcting aerosol sampling instrument data (i.e. a direct solution to the canonical 'inverse' problem of aerosol sampling theory), the present results can also be used to provide preliminary design information for a prospective aerosol sampling system to circumvent the future need for uncomfortably large correction factors (predicted or laboriously measured) in the ambient environment of interest.

The present approach opens the door to several generalizations which will be of practical interest (see, also, Rosner and Tassopoulos, 1990, 1991b)—especially the inclusion of additional deposition and/or coagulation mechanisms, effects of sampling duct bends, variable cross-sectional area, diabatic walls, departures from single-mode log-normality, and the presence of suspended particulate aggregates. Several of these extensions, beyond the scope of this introductory presentation but of importance in sampling from combustion turbines, rockets, and stationary fossil energy power plants (necessarily only briefly discussed in section 6), will be the subject of future communications from this laboratory.

Acknowledgements—This research was supported, in part, by AFOSR (Grant 89-0223), DOE-PETC (Grant DE-FG-2290PC90099), as well as the Yale HTCRE Laboratory Industrial Affiliates (SCM-Corporation, DuPont, Shell, GE and Union Carbide Corporations). It is also a pleasure to acknowledge helpful discussions and/or correspondence with J. Fernandez de la Mora, M. B. Colket, S. Grinshpun, A. G. Konstandopoulos, L. J. Forney and S. W. Rosner.

REFERENCES

Abuzucid, S., Busnaina, A. A. and Ahmadi, G. (1990) Wall deposition of aerosol particles in a turbulent channel flow. *J. Aerosol Sci.*

Bai, H. and Biswas, P. (1990) Diffusional deposition of continuous size distribution aerosols. *J. Aerosol Sci.* **21,** 629–640.

Belyaeu, S. P. and Levin, L. M. (1974) Techniques for collection of representative aerosol samples. *J. Aerosol Sci.* **5,** 325–338.

Biswas, P., Jones, C. L. and Flagan, R. C. (1987) Distortion of size distributions by condensation and evaporation in aerosol instruments. *Aerosol Sci. Technol.* **7,** 231–246.

Biswas, P., Li, X. and Pratsinis, S. E. (1989) Optical waveguide preform fabrication: silica formation and growth in a high temperature aerosol reactor. *J. appl. Phys* **65,** 2445–2450.

Butt, J. B. (1980) *Reaction Kinetics and Reactor Design.* Prentice-Hall, Englewood Cliffs, New Jersey.

Chow, K. H. and Lee, P. S. (1982) *Atmos. Envir.* **16,** 1513–1522.

Cohen, E. R. and Vaughan, E. U. (1971) Approximate solution of the equations for aerosol agglomeration. *J. Colloid Interf. Sci.* **35,** 612–623.

Colket, M. B., Stefucza, J. M., Peters, J. E. and Mellor, A. M. (1977) Radiation and smoke from gas turbine flames, U. S. Army Tank Automotive Command Propulsion Systems Lab (Warren MI) Tech. Report 12163; see, also, *J. Energy (AIAA)* **1,** 115.

Cooper, D. W. and Wu, J. J. (1990) The inversion matrix and error estimation in data inversion: application to diffusion battery measurements. *J. Aerosol Sci.* **21,** 217–226.

Davies, C. N. (1966) Deposition from moving aerosols, chap. 7 in *Aerosol Science* (Edited by Davies, C. N.), pp. 293–446. Academic Press, London.

Davies, C. N. (1968) The entry of aerosols into sampling tubes and heads. *Brit. J. Appl. Physics–J. Phys. D.* **1,** 921.

Denbigh, K. G. and Turner, J. C. R. (1971) *Chemical Reactor Theory,* second edition. Cambridge Univ. Press, Cambridge.

Dobbins, R. A. and Megaridis, C. (1987) Morphology of flame-generated soot as determined by thermophoretic sampling. *Langmuir (ACS)* **3,** 254.

Dobbins, R. A. and Mulholland, G. W. (1984) Interpretation of optical measurements of flame generated particles. *Combust. Sci. Technol.* **40,** 175–191.

Flagan, R. C. and Seinfeld, J. H. (1988) *Fundamentals of Air Pollution Engineering.* Prentice-Hall, Englewood Cliffs, New Jersey.

Frenklach, M. and Harris, S. (1987) Aerosol dynamics modeling using the method of moments. *J. Colloid Interf. Sci.* **118,** 252 (General Motors Res. Lab. Public. GMR-5504, 13 August 1986).

Friedlander, S. K. (1977) *Smoke, Dust and Haze.* John Wiley, New York.

Friedlander, S. K. and Wang, C. S. (1966) The self-preserving particle size distribution for coagulation by Brownian motion–small particle slip correction and simultaneous shear flow. *J. Colloid Interf. Sci.* **22,** 126–132.

Friedlander, S. K. and Wang, C. S. (1967) The self-preserving particle size distribution for coagulation by Brownian motion—small particle slip correction and simultaneous shear flow. *J. Colloid Interf. Sci.* **24,** 170–179.

Fuchs, N. A. (1964) *Mechanics of Aerosols.* Pergamon Press, London.

Fuchs, N. A. and Sutugin, A. G. (1971) Highly dispersed aerosols. In *Topics in Current Aerosol Research* (Edited by Hidy, G. M. and Brock, J. R.), pp. 1–60. Pergamon Press, Oxford.

Hidy, G. (1984) *Aerosols—An Industrial and Environmental Science.* Academic Press, New York.
Hinds, W. C. (1982) *Aerosol Technology—Properties, Behavior and Measurement of Airborne Particles.* John Wiley, New York.
Huebert, B. J., Lee, G. and Warren, W. L. (1990) Airborne aerosol inlet passing efficiency measurement. *J. Geophys. Res.* **95,** 16,369–16,387.
Hungal, S. and Willeke, K. (1990) Aspiration efficiency: unified model for all sampling angles. *Envir. Sci. Technol.* **24,** 688–691.
Ivie, J. J., Forney, L. J. and Roach, R. L. (1990) Supersonic particle probes: measurement of internal wall losses. *Aerosol Sci. Technol.* **13,** 10.
Lai, F. S., Friedlander, S. K., Pich, J. and Hidy, G. M. (1971) The self-preserving particle size distribution for Brownian coagulation in the free-molecule regime. *J. Colloid Interface Sci.* **39,** 395–405.
Landgrebe, J. D. (1989) Gas-phase particulate manufacture: the interplay of chemical reaction and aerosol coagulation. MS Dissertation. Univ. of Cincinnati, Dept. ChE/Nuclear Eng.
Landgrebe, J. D., Pratsinis, S. E. and Mastrangelo, S. V. R. (1990) Nomographs for vapor synthesis of ceramic powders. *Chem. Eng. Sci.* **45,** 2931–2941.
Lee, K. W., Chen, H. and Gieseke, J. A. (1984) Log-normality preserving size distribution for Brownian coagulation in the free-molecule regime. *Aerosol Sci. Technol.* **3,** 53–62.
Liu, B. Y. H. and Agarwal, J. K. (1974) Experimental observations of aerosol deposition in turbulent pipe flow. *J. Aerosol Sci.* **5,** 145–155.
Mackowski, D. W., Tassopoulos, M. and Rosner, D. E. (1991) Effect of radiative heat transfer on the coagulation rates of combustion-generated particulates. Combustion Inst-Central States Section, Spring Meeting 21–24 April 1991, Nashville, TN.
Megaridis, C. M. (1987) Thermophoretic sampling and soot aerosol dynamics of an ethene diffusion flame, PhD Dissertation, Brown Univ., Providence, RI; see, also NBS-(now NIST-) Report NBS-GCR-87-532.
Megaridis, C. M. and Dobbins, R. A. (1989) An integral solution of the aerosol dynamic equation including surface growth reactions. *Comb. Sci. Technol.* **63,** 153–167.
Megaridis, C. M. and Dobbins, R. A. (1990a) A bimodal integral solution of the dynamic equation for an aerosol undergoing particle inception and coagulation. *Aerosol Sci. Technol.* **12,** 240–255.
Megaridis, C. M. and Dobbins, R. A. (1990b) Morphological description of flame-generated materials. *Comb. Sci. Technol.* **71,** 95–109.
Mercer, T. T. (1973) *Aerosol Technology in Hazard Evaluation.* Academic Press, New York.
Mercer, T. T. and Greene, T. D. (1974) Interpretation of diffusion 'battery' data. *J. Aerosol Sci.* **5,** 251–255.
Mitchell, J. P., Edwards, R. T. and Ball, M. H. E. (1989) The penetration of aerosols through fine capillaries. Atomic Energy Authority Report AEEW-R-2558. Winfrith, U.K.
Ohadi, M. M. and Sparrow, E. M. (1989) Heat transfer in a straight tube situated downstream of a bend. *Int. J. Heat Mass Transfer* **32,** 201–212.
Park, H. M. and Rosner, D. E. (1989) Boundary layer coagulation effects on the size distribution of thermophoretically deposited particles. *Chem. Eng. Sci.* **44,** 2225–2231.
Pratsinis, S. E. and Kim, K. S. (1989) Particle coagulation, diffusion and thermophoresis in laminar tube flows. *J. Aerosol Sci.* **20,** 101–111.
Probstein, R. (1989) *Physicochemical Hydrodynamics—An Introduction.* Butterworth-Heinemann, Stoneham, Massachusetts.
Rosner, D. E. (1986) *Transport Processes in Chemically Reacting Flow Systems.* Butterworth-Heinemann, Stoneham, Massachusetts.
Rosner, D. E. (1989) Total mass deposition rates from 'polydispersed' aerosols. *AIChE J.* **35,** 164–167.
Rosner, D. E. (1991) Structure-sensitivity of total mass deposition rates from streams containing coagulation-aged populations of aggregated primary particles (in preparation).
Rosner, D. E. and Tassopoulos, M. (1989) Deposition rates from 'polydispersed' particle populations of arbitrary spread. *AIChE J.* **35,** 1497–1508.
Rosner, D. E., Konstandopolous, A. G., Tassopoulos, M. and Mackowski, D. W. (1991) Deposition dynamics of combustion-generated particles: summary of recent studies of particle transport mechanisms, capture rates and resulting deposit microstructure/properties, Proc. Engineering Foundation Conference: *Inorganic Transformations and Ash Deposition During Combustion* (in press).
Rosner, D. E., Mackowski, D. W., Tassopoulos, M., Castillo, J. and Garcia-Ybarra, P. (1990) Effects of heat transfer on the dynamics and transport of small particles in gases, I/EC-Research (in press). (Paper 293e AIChE 1990 Annual Mtg., Chicago, IL, 12 Nov.).
Rosner, D. E. and Tassopoulos, M. (1990) Moment methods to predict coagulation effects on deposition rate phenomena, Paper 5E.5, 1990 Meeting of the Amer. Assoc. Aerosol Res., 18–22 June, Philadelphia, PA.
Rosner, D. E. and Tassopoulos, M. (1991a) Moment method calculation of mass transfer entrance effects on wall-loss corrections in laminar flow aerosol sampling systems (in preparation).
Rosner, D. E. and Tassopoulos, M. (1991b) Moment methods in the theory of 'polydispersed' particle deposition from flowing suspensions. (in preparation.)
Rosner, D. E. *et al.* (1991) Use of available sublimation, electrochemical and heat transfer data to estimate ultrafine particle losses in sampling systems containing bends. Yale Univ. HTCRE Lab. Publication (in prep.).
Seinfeld, J. H. (1986) *Air Pollution.* Wiley, New York.
Sparrow, E. M. and Chrysler, G. M. (1986) Turbulent flow and heat transfer in bends of circular cross-section. *ASME Trans.-J. Heat Trans.* **108,** 40–47.
Ulrich, G. D. and Riehl, J. W. (1982) Aggregation and growth of submicron oxide particles in flames. *J. Colloid Interface Sci.* **87,** 257.
Ulrich, G. D. and Subramanian, N. S. (1977) Particle growth in flames, III. Coalescence as a rate-controlling process. *Comb. Sci. Technol.* **17,** 119–126.
Vincent, J. H. (1989) *Aerosol Sampling and Practice,* chap. 10. John Wiley, Chichester.

Zachariah, M. and Semerjian, H. (1989) Simulation of ceramic particle formation: comparison with *in situ* measurements. *AIChE J.* **35**, 2003–2012.
Zebel, Z. (1978) Some problems in the sampling of aerosols. In *Recent Developments in Aerosol Science* (Edited by Shaw, D. T.). Wiley-Interscience, New York.

APPENDIX A: $C_2^{(k)}$ COEFFICIENTS

In this Appendix we provide the second-order terms, $C_2^{(k)}$†, of the small-ξ expansions (see equation (27)). The wall-loss (WL) terms, clearly the same for free-molecule and continuum coagulation, are:

$$\tilde{N}''_{p,WL}(L)=\left[b\tilde{\phi}'_p+(1-b)\tilde{N}'_p+\frac{(b-1)b(-2\tilde{\phi}'_p+\tilde{M}'_2+\tilde{N}'_p)}{2}\right]_L$$

$$\tilde{\phi}''_{p,WL}(L)=\left[-(1+b)[\tilde{\phi}'_p]^2+b\tilde{N}'_p\tilde{\phi}'_p-\frac{(b-1)b(-2\tilde{\phi}'_p+\tilde{N}'_p+\tilde{M}'_2)\tilde{\phi}'_p}{2}\right]_L$$

$$\tilde{M}''_{2,WL}(L)=\left[b(\tilde{\phi}'_p-\tilde{N}'_p)+\tilde{M}'_2+\frac{b(3+b)(-2\tilde{\phi}'_p+\tilde{M}'_2+\tilde{N}'_p)}{2}\right]_L\cdot\exp(2b\ln^2\sigma_{g,L}),$$

where $\tilde{N}'_p$, $\tilde{\phi}'_p$ and $\tilde{M}'_2$ are the first-order expansion coefficients* defined in equations (28). Next we provide the coefficients associated with coagulation†. For free-molecule coagulation we find:

$$\tilde{N}''_{p,C}(L)=\left[\frac{1}{6}\tilde{\phi}'_p+2\tilde{N}'_p+\frac{5(-2\tilde{\phi}'_p+\tilde{M}'_2+\tilde{N}'_p)}{48}\right]_L\cdot\frac{C}{(\ln\sigma_{g,L})^{1/3}\exp(\frac{1}{12}\ln^2\sigma_{g,L})}$$

$$\tilde{\phi}''_{p,C}(L)=0$$

$$\tilde{M}''_{2,C}(L)=C\cdot\left\{-\frac{2\left[\frac{13}{6}\tilde{\phi}'_p+2\tilde{N}'_p+\frac{13}{48}(-2\tilde{\phi}'_p+\tilde{N}'_p+\tilde{M}'_2)\right]_L}{(\ln\sigma_{g,L})^{13/3}\cdot\exp\left(\frac{37}{12}\ln^2\sigma_{g,L}\right)}\right\}.$$

The corresponding coefficients for continuum coagulation are:

$$\tilde{N}''_{p,C}(L)=C\cdot\frac{2[1+\exp(\frac{1}{9}\ln^2\sigma_{g,L})]\tilde{N}'_p+\frac{1}{9}\exp(\ln^2\sigma_{g,L})(-2\tilde{\phi}_p+\tilde{M}'_2+\tilde{N}'_p)}{1+\exp(\frac{1}{9}\ln^2\sigma_{g,L})}$$

$$\tilde{\phi}''_{p,C}(L)=0$$

$$\tilde{M}''_{2,C}(L)=C\left\{-\frac{2\left[2\left(1+\exp\left(\frac{1}{9}\ln^2\sigma_{g,L}\right)\right)+\frac{1}{9}\exp(\ln^2\sigma_{g,L})(-2\tilde{\phi}_p+\tilde{M}'_2+\tilde{N}'_p)\right]}{\exp(\ln^2\sigma_{g,L})\cdot[1+\exp(\ln^2\sigma_{g,L})]}\right\}.$$

These coefficients can prove useful to evaluate correction factors when ξ_{max} exceeds, say 0.2, but does not exceed about 0.6. For values of ξ_{max} much above 0.6 direct use should be made of the figures of section 4.2 or specific numerical integrations in accord with section 4.3.

* In the present notation $C_1^{(0)}\equiv\tilde{N}_{p,L}$, $C_1^{(1)}\equiv\tilde{\phi}'_{p,L}$, $C_1^{(2)}\equiv\tilde{M}'_{2,L}$.
† Note that $C_2^{(0)}\equiv\tilde{N}''_{p,WL}(L)+\tilde{N}''_{p,C}(L)$, etc.